water

MDPI

Article

Competitive Adsorption of Drugs from a Multi-Component Mixture on Sugarcane Bagasse

Maria E. Peñafiel [1,*] and Damián Flores [2]

[1] Grupo de Ingeniería de Reactores, Catálisis y Tecnologías del Medio Ambiente, Departamento de Biociencias, Universidad de Cuenca, Avenida Víctor Manuel Albornoz, Cuenca 010202, Ecuador
[2] Facultad de Ciencias Químicas, Universidad de Cuenca, Cuenca 010202, Ecuador; damian.flores@ucuenca.edu.ec
* Correspondence: maria.penafiel@ucuenca.edu.ec; Tel.: +593-991475901

Abstract: This work examines the adsorption in single- and multi-solute adsorption experiments of antibiotic and non-steroidal anti-inflammatory drugs, i.e., ciprofloxacin (CPX), sulfamethoxazole (SMX), ibuprofen (IBU), and diclofenac (DCF), onto sugarcane bagasse. The maximum experimental adsorption capacities of single components CPX, DCF, IBU, and SMX, were 0.98, 0.77, 0.61, and 0.51 mg/g, respectively, with decreases between 5 and 28% in multi-solute mixtures, assuming competitive adsorption. The experimental data of a single drug fitted a pseudo-second-order model, while the experimental isotherms fit the Freundlich model. The presence of CPX did not interfere with the adsorption of other solutes. The adsorption of SMX was lower in the presence of adsorption competitors than SMX single solution. The adsorption of binary systems adequately fitted the Sheindorf–Rebhun–Sheintuch model. The results showed that the competition process depends on each adsorbate and that sugarcane bagasse can adsorb drugs in multi-component systems.

Keywords: competitive adsorption; diclofenac; ciprofloxacin; ibuprofen; sulfamethoxazole; sugarcane bagasse

check for updates

Citation: Peñafiel, M.E.; Flores, D. Competitive Adsorption of Drugs from a Multi-Component Mixture on Sugarcane Bagasse. *Water* **2023**, *15*, 2127. https://doi.org/10.3390/w15112127

Academic Editors: Sílvia Santos, Ariana Pintor and Antonio Turco

Received: 8 May 2023
Revised: 22 May 2023
Accepted: 23 May 2023
Published: 3 June 2023

1. Introduction

Pharmaceuticals such as antibiotics, analgesics, anti-inflammatories, and others improve life and reduce mortality caused by diseases. Thus, a wide variety of drugs enter the wastewater and natural water because of their manufacture and use in medicine and veterinary medicine. Their continuous administration has provoked a widespread occurrence of pharmaceuticals in natural aquatic ecosystems, with antibiotics and anti-inflammatory drugs being prevalent drugs [1–5].

The occurrence of drugs in water and their possible toxicity to human and environmental health has guided researchers to investigate effective treatments to eliminate them [6–8]. One of the most suitable methods for micropollutant removal from aqueous solution is adsorption because it is effective at low concentrations and is cheap, but the nature of the adsorbent has an influence, especially its abundance and low cost. Previous works by our research group and other studies reported that some agro-industrial residues have proven to be efficient in adsorbing single-solute pharmaceuticals [9–11]. However, as stated by Silva et al. [8], most studies investigate the elimination of a single component without considering the interaction of other drugs, which is why multi-component studies are essential. Other researchers argue that the use of agricultural residues as adsorbents can reduce the costs of the process, giving economic value to the waste and helping to protect the environment. Therefore, the use of sugarcane bagasse residue would provide an abundant and low-cost adsorbent [10].

Although Sharma et al. [12] warn of the risks to health and the environment derived from exposure to mixtures of emerging pollutants, to our knowledge, there is a lack of studies on the competitive adsorption process in the presence of other pharmaceuticals in

multicomponent solutions. The influence of a component on the adsorption capacity of another depends on the interactions between them; the interactions between antibiotics and anti-inflammatory drugs have been less studied and are well worth greater exploration. In addition, these few studies used manufactured materials such as activated carbon and nanomaterials [13–16]. Our work proposes natural materials such as agricultural waste as a promising way to find low-cost and easily used adsorbents.

In this work, the competitive adsorption of two anti-inflammatory drugs, diclofenac (DFC) and ibuprofen (IBU), and two antibiotics, ciprofloxacin (CPX) and sulfamethoxazole (SMX), on untreated sugarcane bagasse was investigated to determine the influence of simultaneous adsorption.

Sulfamethoxazole (SMX) and ciprofloxacin (CPX) are the most frequently detected antibiotics. CPX is the most prescribed human antibiotic, while SMX is largely used in veterinary medicine [2,17]. These two antibiotics have demonstrated very high toxicity to cyanobacteria and freshwater algae [17]. The propagation of antibiotics in the water and environment is a world health problem due to microbial resistance and potential bioaccumulation. Although the problem of microbial resistance is attributed to the abundance and undue utilization of antibiotics, the contamination of surface water and drinking water with these types of compounds can further aggravate this situation [18,19].

On the other hand, anti-inflammatories are widely prescribed and sold over the counter. Anti-inflammatories such as IBU and DCF occur in wastewater and natural waters; their toxicity has been reported due to bio-accumulation in the blood plasma of fish, altering the functioning of the liver and kidneys and causing a significant deterioration in health [20,21]. The antibiotic CPX and the anti-inflammatory DCF were selected because they are on the watch list of the European Union (EU Decision, 2018/940 of 5 June 2018).

Consequently, the objectives of this work were to (i) compare the adsorption capacity of SB to adsorb CPX, SMX, DCF, and IBU in single, binary, ternary, and quaternary mixtures; (ii) investigate which drugs affect the adsorption capacity of the others and why; and (iii) show that SB, an agricultural waste, has value as an adsorbent for emerging pollutants.

Theory

In a multi-component solution that has more than one adsorbable constituent, the constituents will compete for available adsorption sites on the adsorbent surface. The amount of single solute adsorbed to equilibrium ($q_{e,}i$), of a component depends on its concentration ($C_{e,}i$), and the concentrations of all other components. For a mixture of N adsorbates, the following relationships hold [22].

$$\begin{aligned} q_{e,}1 &= f(C_e1,\ C_e2,\ C_e3,\ \ldots\ \ldots\ \ldots,\ C_eN) \\ q_{e,}2 &= f(C_e1,\ C_e2,\ C_e3,\ \ldots\ \ldots\ \ldots,\ C_eN) \\ q_{e,}3 &= f(C_e1,\ C_e2,\ C_e3,\ \ldots\ \ldots\ \ldots,\ C_eN) \\ q_{e,}N &= f(C_e1,\ C_e2,\ C_e3,\ \ldots\ \ldots\ \ldots,\ C_eN) \end{aligned} \quad (1)$$

The isotherms of each component in multicomponent solutions can be determined in the same way as that described for single solute adsorption. The adsorption capacity of each component in an N-component system and the total amount of solute adsorbed on the adsorbent follow the equations.

$$q_{e,i} = \frac{(C_{o,i} - C_{e,i})V}{m} \quad i = 1 \ldots N \quad (2)$$

$$q_{e,T} = \sum_{i=1}^{N} q_{e,i} \quad (3)$$

where $q_{e,i}$ and $q_{e,T}$ are the equilibrium adsorption capacity of each component and the total adsorption capacity, respectively, (mg/g) $C_{o,i}$ and $C_{e,i}$ are the initial and equilib-

rium concentrations of drugs (mg/L) V is the volume of solution (L), and m is the mass of bagasse (g).

Several models have been proposed for the study of competitive adsorption. Butler and Ockrent (1930) developed the extended Langmuir equation. This model neglects the interactions and assumes that the only effect for the decrease of the amount of component A adsorbed is the reduction of the vacant active sites on the adsorbent surface due to the adsorption of other components.

$$q_i = \frac{q_{m,i} K_i C_{e,1}}{1 + \sum_{j=1}^{N} K_j C_j} \quad (4)$$

where $q_{m,i}$ the maximum adsorption capacity of each component (mg/g); K_i is the Langmuir constant. $q_{m,i}$ and K_i for each component are the same as for the single solute isotherm equation.

DiGiano et al. [23] developed an isotherm for N components based on the Freundlich model assuming that all components have the same value of the exponent, n, and differ only in coefficients, $K_{F,i}$.

$$q_i = \frac{K_{F,i}^{1/n} C_{e,i}}{\left(\sum_{j=1}^{N} K_{F,j}^{\frac{1}{n}} C_{ej}\right)} \quad (5)$$

Sheindorf–Rebhun–Sheintuch (SRS) proposed an extension of the Freundlich isotherm for bicomponent adsorption based on the assumption that an exponential distribution of adsorption energies exists for each component. In this model, each component individually must obey the Freundlich isotherm $K_{F,i}$ [24].

$$q_i = K_{F,i} C_{e,i} \left(\sum_{j=1}^{N} \alpha_{i,j} C_{e,j}\right)^{n_i - 1} \quad (6)$$

q_i is the adsorption capacity of component i in the presence of component j (mg/g); $C_{e,i}$ and $C_{e,j}$ are the equilibrium concentrations of component i and j, respectively (mg/L). $K_{F,i}$ is the single-component Freundlich adsorption capacity parameter for component i (L/g). n_i is the Freundlich adsorption intensity parameter for component i. $\alpha i,j$ is the competitive coefficient. These data are determined from experimental data of bicomponent systems. The values for αij range from zero (complete lack of competition) to values greater than zero (normally < 10) for a high degree of competition [25].

2. Materials and Methods

2.1. Adsorbent—Sugarcane Bagasse

Untreated sugarcane bagasse (Figure 1) was used as an adsorbent; it was only washed with ultrapure water, dried in an oven (60 °C for 8 h), and ground. The triturate residue has a size particle of less than 0.4 mm. The characterization of sugarcane bagasse used in this work was presented in previous work [10].

2.2. Adsorbates—Drugs

Sulfamethoxazole (SMX), ciprofloxacin (CPX), ibuprofen (IBU), and diclofenac (DCF) of analytical grade supplied by Sigma Aldrich (Product by St. Louis, MO, USA) were used. The physical and chemical characteristics of the pharmaceuticals are described in Table 1. Their molecular structure is shown in Figure 2. Peñafiel et al. [10] presented a method to prepare single-component solutions. The multi-component solutions were prepared by adding the necessary amount of each drug to ultrapure water.

Figure 1. Untreated and ground sugarcane bagasse.

Table 1. Physical and chemical characteristics of the drugs.

Drug	Class	Molecular Weight ($g \cdot mol^{-1}$)	Log K_{ow}	Dissociation Constant (pKa)	Size (nm)	Λ_{max} (nm)
IBU	Analgesic	206.28	3.97	4.5	1.39 × 0.73 [26]	222
CPX	Antibiotic	331.34	0.28	6.0–8.7	0.825 [27]	271
DCF	Analgesic	318.10	5.71	4.2	0.97 × 0.96	276
SMX	Antibiotic	253.28	0.89	1.9–5.7	0.56 × 1.03	261

Note: Λ_{max}: wavelength.

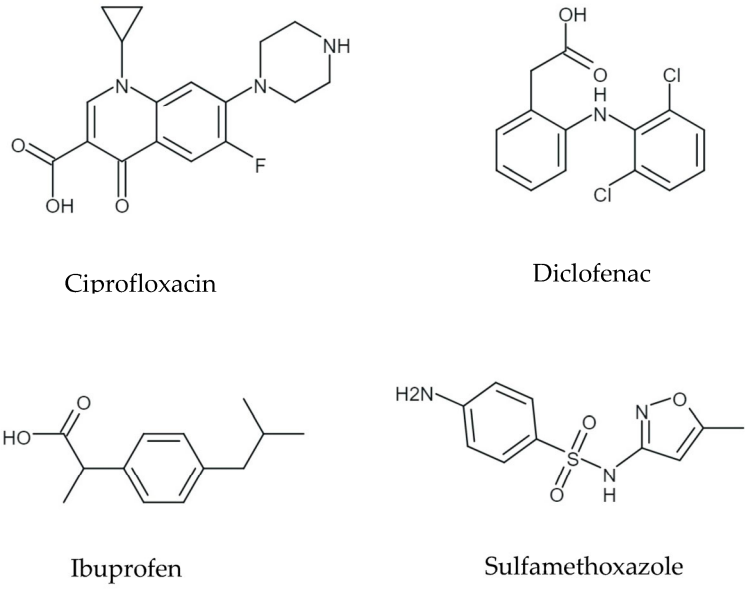

Figure 2. Molecular structure of the drugs.

2.3. Adsorption Experiments for Single- and Multi-Component Drug Solutions

Some tests were carried out to study the adsorption of single components and multi-component mixtures. For this, 50 mL of a solution of single and multi-component drugs was added to 1 g of sugarcane bagasse as adsorbent in a batch process in a Thermo Scientific™ MaxQ™ 4000 (Waltham, MA, USA) orbital shaker, at 150 rpm, pH 6.5, and 20 °C. The kinetics and equilibrium of the adsorption process were studied.

For the kinetic experiments, solutions of 20 mg/L were shaken for 120 min to reach adsorption equilibrium. The time to reach equilibrium was tested at intervals of 2, 5, 10, 20, 30, 40, 60, 100, and 120 min. The effect of the drug concentration was observed by varying initial concentrations between 10 and 60 mg/L for 100 min. High-performance

liquid chromatography determined the concentration of drugs. The High-Performance Liquid Chromatography (HPLC) procedure is shown in the Supplementary Materials. The amount of each drug adsorbed was calculated as

$$q_e = \frac{(C_o - C_e)V}{m} \quad (7)$$

where C_o and C_e, are the initial and equilibrium concentrations of drugs (mg/L), V is the volume of the solution (L), and m is the mass of bagasse (g).

The kinetic and equilibrium models used to fit the experimental data of single-component adsorption were the pseudo-first-order and pseudo-second-order models and the Langmuir and Freundlich models, respectively. Linearized equations of all models were used.

$$\text{Pseudo-first-order} \quad \ln(q_e - q_t) = \ln q_e - K_1 t \quad (8)$$

$$\text{Pseudo-second-order} \quad \frac{t}{q_t} = \frac{1}{K_2 q_e^2} + \frac{t}{q_e} \quad (9)$$

$$\text{Langmuir} \quad \frac{C_e}{q_e} = \frac{C_e}{q_m} + \frac{1}{K_L q_m} \quad (10)$$

$$\text{Freundlich} \quad \log q_e = \log k_F - \frac{1}{n} \log C_e \quad (11)$$

where C_e is the concentration of the solution (mg/L); q_e is the equilibrium adsorption capacity, and q_t is the adsorption capacity at any time (mg/g); K_1 and K_2 represent the pseudo-first-order and pseudo-second-order rate constants; q_m is the maximum adsorption capacity (mg/g); K_L is the Langmuir constant (L/mg); K_F is the Freundlich constant, (mg/L) $(\text{mg/g})^{-\frac{1}{n}}$; n refers to the adsorption intensity (dimensionless).

2.4. Characterization of Adsorbents

The SB used in this competitive adsorption was characterized in previous work. The specific surface area, pore size, surface morphology, functional groups on the surface, and point of zero charges were determined. Each method is described in Peñafiel et al. [10]. The molecular structure of SB, cellulose, lignin, and the hemicellulose content were determined using TAPPI standards (Technical Association of the Pulp and Paper Industry, 1978).

2.5. Statistics Analysis

All tests were performed in triplicate, and standard deviations (SD) were calculated. The best fit of the experimental data of an equation model was determined by the regression correlation coefficient (R^2). The error between the experimental and the predicted values of the model was evaluated using Marquardt's percent standard derivation (MPSD):

$$\text{MPSD} = 100 \sqrt{\frac{1}{n - N} \left(\sum_{i=1}^{p} \left[\left(q_{exp} - q_{cal} \right) / q_{exp} \right]^2 \right)} \quad (12)$$

where p is the number of experimental data points and N is the parameter of the model equation; q_{exp} and q_{cal} are the experimental and calculated capacity, respectively.

3. Results

3.1. Characterization of Sugarcane Bagasse

Table 2 shows the properties of SB. Figure 3 shows the SEM image. The surface of the SB is very smooth with few large pores, which confirms its macroporosity [9].

Table 2. Physical and chemical characteristics of SB [10].

Properties	
S_{BET} (m^2 g^{-1})	2.5
Desorption average pore diameter (nm)	10.6
pH_{PZC}	6.1

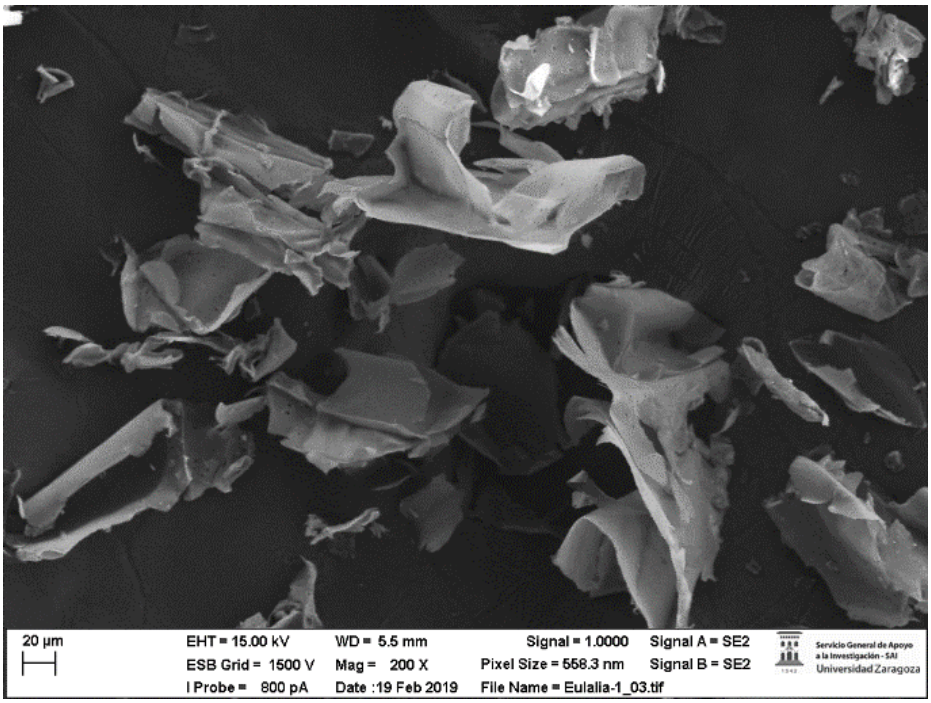

Figure 3. SEM images of the surface of SB.

The SB used in this work contains 44.5% cellulose, 32.9 hemicellulose, and 19.2% lignin. These values are similar to those in other works, such as Varma and Mondal et al., and Carrier et al. [28,29]. The chemical characteristics of SB can be seen in [10]. According to several works, lignin presents adsorptive properties [29–31]. However, the relationship between the adsorbent properties and the lignin content could not be determined.

3.2. Kinetic Studies for Single Components

The amount of SB to be used in the competitive multi-component adsorption was determined by the dose of SB necessary to achieve the maximum elimination percentage of a single drug. Each drug achieved its maximum removal percentage with different amounts of SB. Adsorption percentages of 51 and 65% were reached with 20 mg/L of SB for SMX and IBU, respectively. A dose of 5 g/L of SB removed 99% of CPX. The DCF reached a maximal removal of 77% with 17 mg/L of SB. Consequently, 20 mg/L of SB was used for multiple-component adsorption. The results are shown in Figure S1.

The adsorption proceeded rapidly, reaching around 70% of the total adsorbed solute in the first 5 min, as can see in Figure 4. All drugs reached equilibrium at 60 min, showing a significant difference with other adsorbents such as activated carbons that reached equilibrium in longer periods.

The rapid adsorption was due to the mesoporosity and macroporosity of the bagasse. The macroporosity of SB allows easy access to drugs with molecular lengths smaller than the average diameter of the bagasse pores (SMX, 056 × 1.03 nm; CPX, 0.826 × 0.98 nm; DCF, 0.97 × 0.95 nm; IBU 1.03 × 0.52 nm) [10,32].

Figure 4a–d show the experimental data fitted to the pseudo-first-order and pseudo-second-order models for each single solute. The best fit for each drug was with the

pseudo-second-order model, with R^2 values of 0.99. The pseudo-first-order model fit was unfavorable, as shown in Table 3.

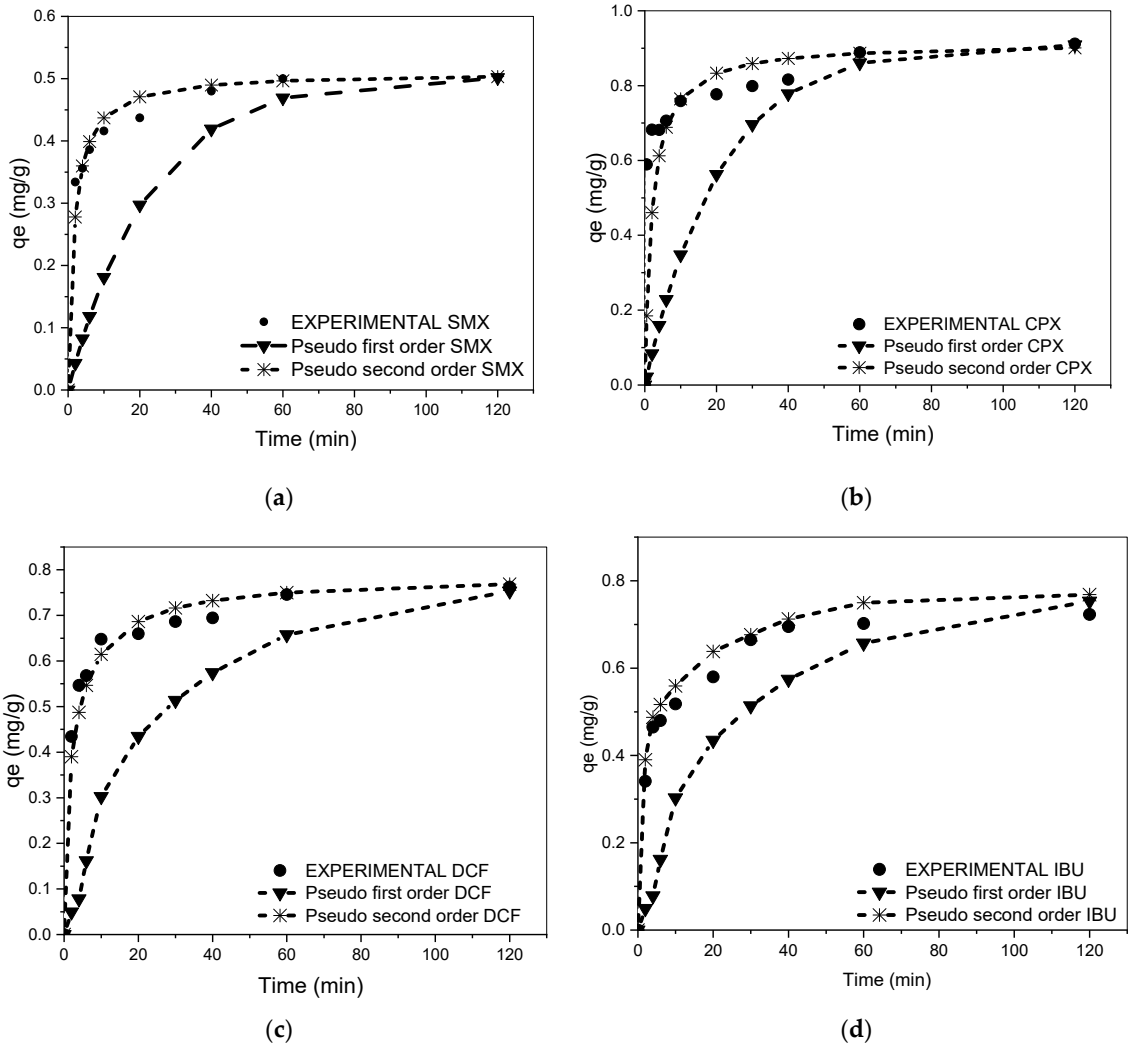

Figure 4. Fitted the data of the pseudo-first-order and pseudo-second-order models. (**a**) SMX, (**b**) CPX, (**c**) DCF, and (**d**) IBU.

Table 3. Parameters of experimental data and pseudo-first-order and pseudo-second-order models.

Drug	q_e exp ($mg \cdot g^{-1}$)	Pseudo-First-Order Models			
		q_e (SD) ($mg \cdot g^{-1}$)	K_1 (min^{-1})	R^2	MPSD
SMX	0.51 (±0.03)	0.50 (±0.02)	0.045	0.77	20.2
CPX	0.98 (±0.01)	0.95 (±0.01)	0.028	0.78	11.7
DCF	0.77 (±0.02)	0.55 (±0.02)	0.026	0.75	14.3
IBU	0.61 (±0.02)	0.64 (±0.03)	0.035	0.82	12.6
Drug	**Pseudo-Second-Order Models**				
	q_e (SD) ($mg \cdot g^{-1}$)	K_2 ($mg \cdot g^{-1} min^{-1}$)	R^2	MPSD	
SMX	0.51 ± (0.02)	1.17	0.99	12.2	
CPX	0.97 ± (0.01)	0.09	0.99	6.7	
DCF	0.78 ± (0.02)	0.40	0.99	8.3	
IBU	0.62 ± (0.03)	0.98	0.98	10.6	

Note: SD = standard deviation; MPSD = Marquardt's percent standard deviation.

3.3. Equilibrium Adsorption Isotherm for Single Solutes

The equilibrium study was conducted for 100 min at 20 °C, and the solution concentration was between 5 and 60 mg/L.

Figure 5a–d show that the isotherms of all drugs are similar. The isotherms correspond to the Giles L3 type [33], indicating favorable adsorption with multilayer formation, which had already been seen in previous works [9,10]. The steep slope of the initial part of the isotherm evidences the affinity between drugs and residues. The decrease in the initial slope is due to the difficulty of the solute to find active sites on the adsorbent when its concentration increases, mainly due to the competition between the adsorbate and the solvent [33,34]; the subsequent increase in the slope indicates the formation of a multilayer since the adsorbed molecules facilitate the adsorption of new molecules by an adsorbate–adsorbate relationship.

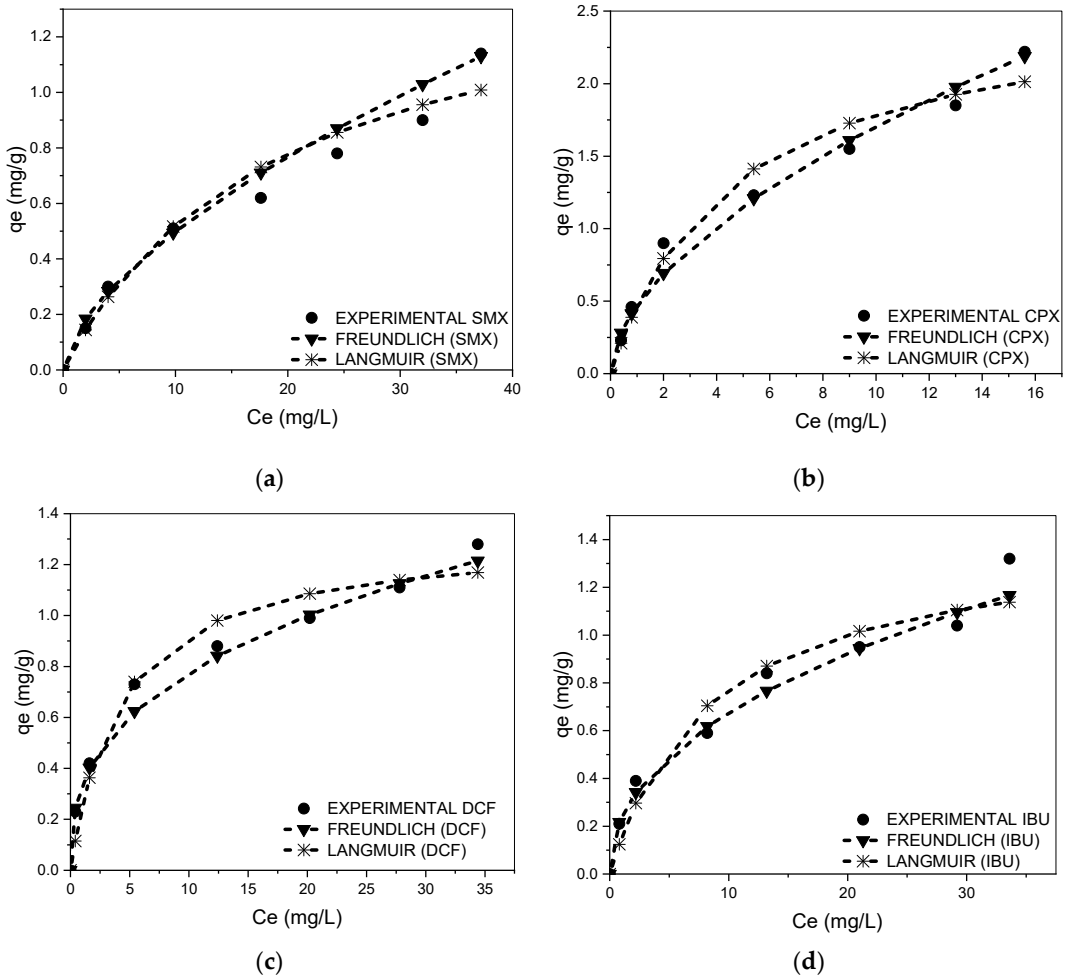

Figure 5. Experimental isotherm and adjusted Langmuir and Freundlich models. (**a**) SMX, (**b**) CPX, (**c**) DCF, and (**d**) IBU. (20 °C, pH 6.5).

The Langmuir and Freundlich models were applied to compare the monolayer adsorption with the multilayer adsorption-based model. The coefficients of the experimental data of the Langmuir and Freundlich models are shown in Table 4. The Freundlich model better describes the behavior of drug adsorption on residues (Figure 5) since its correlation coefficient (R^2) is higher.

Table 4. Parameters of the adsorption models for the Langmuir and Freundlich isotherms.

Drug	Langmuir				Freundlich			
	q_m (SD)	K_L	R^2	MPSD	K_F	n	R^2	MPSD
	(mg·g^{-1})	(L·mg^{-1})			(mg/g) (mg/L)$^{-1/n}$			
SMX	1.43 (±0.08)	0.05	0.90	18.5	0.12	1.53	0.98	8.5
CPX	2.61(±0.12)	0.22	0.94	7.5	1.47	1.78	0.98	5.6
DCF	1.81(±0.09)	0.24	0.96	12.5	0.34	2.78	0.98	10.2
IBU	1.62(±0.09)	0.12	0.93	23.2	0.24	2.22	0.98	13.2

Note: SD = standard deviation; MPSD = Marquardt's percent standard deviation.

The Freundlich equation indicates that the surface of the adsorbent is heterogeneous, and there are active sites of various affinities; firstly, the active sites with greater affinity are filled, and the others are subsequently occupied. This model proposes physical and chemical adsorption between the adsorbate and adsorbent.

The amount of drug adsorbed for a unit equilibrium concentration (K_F) for ciprofloxacin is higher than that for diclofenac, ibuprofen, and sulfamethoxazole, which are similar to each other. For all adsorbed drugs, the value of n indicates favorable processes.

All adsorption capacities are summarized in Table 4. The experimental results of single solutes indicate that CPX is better adsorbed than the other drugs, DCF, SMX, and IBU. The amount of CPX adsorbed is higher than that of the other drugs as follows: CPX > DCF > IBU > SMX. CPX, DCF, IBU, and SMX adsorption reaches a maximum adsorption capacity of 2.61, 1.81, 1.62, and 1.43 mg/g. The results could be attributed to the adsorption of drugs on SB due to the ability to form hydrogen bonds, which is the principal mechanism of the physical adsorption of drugs on agricultural residues [9,10]. The low adsorption of IBU may be due to the smaller molecular structure of IBU that reduces π-π interactions; however, the adsorption capacity of IBU is smaller than that of SMX due to a hydrophobic effect [14]. These results indicate (i) the SB is capable of adsorbing all of the drugs studied, (ii) there are differences in the adsorption capacity that depend on the class and nature of each drug, and (iii) the adsorption mechanisms depend on each drug.

3.4. Competitive Adsorption in Binary, Ternary, and Quaternary Systems

To investigate the involvement of competition in adsorption, binary, ternary, and quaternary solutions with initial concentrations of 20 mg/L were prepared. Figure 6 exhibits the different amounts of drug adsorbed over time for the binary, ternary, and quaternary systems.

The adsorption capacity of CPX remained almost constant in the binary, ternary, and quaternary systems (Figure 6a) decreasing only 5% in ternary and quaternary mixtures. In the presence of the other pharmaceuticals, the CPX adsorption was similar to the system of CPX singly, i.e., 0.98 mg/g, indicating a high affinity for CPX [10]. The time required to reach equilibrium did not vary with the presence of other solutes.

The variation of the SMX adsorption capacity in the presence of other pharmaceuticals is shown in Figure 6b. In the binary system, the adsorption of SMX decreased by approximately 21%, while in the ternary and quaternary systems, the reduction was around 30% and 43%, respectively.

The amount of SMX adsorbed at equilibrium decreased from 0.51 mg/g when it was alone to 0.29 mg/g in quaternary systems. This result is consistent with that presented by Li et al. [15], who affirmed a reduction in SMX adsorption in the presence of another solute. The adsorption of SMX accelerated with the addition of other drugs. The time necessary to reach SMX equilibrium was 45 min. The results show the low affinity of SMX with SB and the difficulty in removing SMX from a multi-component solution.

The amount of single DCF adsorbed decreased to a lesser extent in the presence of other solutes, as can be observed in Figure 6c. The capacity of SB to adsorb DCF decreased

by approximately 10% in quaternary mixtures. Figure 6d shows the IBU adsorption in the presence of other solutes. The adsorption amount of IBU decreased by 10 and 15% in binary and ternary systems, respectively. In quaternary mixtures, the reduction was higher, reaching 17 % at high concentrations (Figure 6d). For both IBU and DCF, the time necessary to reach equilibrium remained the same as that for single components, i.e., 60 min.

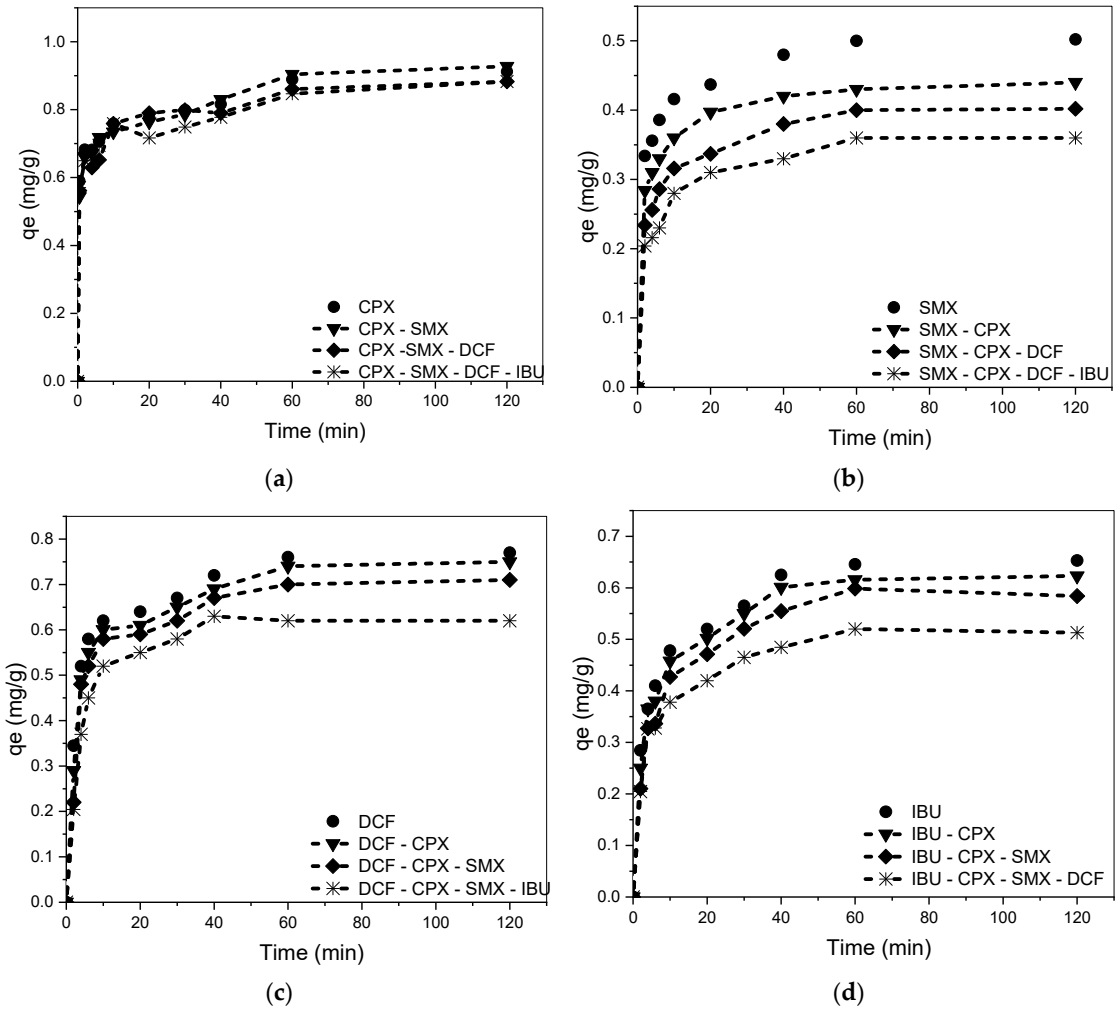

Figure 6. Percentage removal vs. time (pH 6.5; 20 °C). (**a**) CPX as a single component and in mixtures; (**b**) SMX as a single component and in mixtures; (**c**) DCF as a single component and in mixtures; and (**d**) IBU as a single component and in mixtures.

Figure 7a shows the isotherms of SMX in the presence of other drugs. A decrease in the SMX adsorption in all studied simultaneous systems capacity can be observed. Figure 7b shows the influence of CPX, DCF, and IBU on the adsorption of SMX. The amounts of SMX adsorbed on SB in the binary system decreased as follows: SMX singly > SMX with CPX > SMX with DCF > SMX with IBU. CPX had a lesser influence on the adsorption of SMX. The adsorption capacity decreased from 0.51 to 0.49, which was due to the lower amount of SB required for CPX adsorption, leaving free active sites for SMX. The presence of DFC reduced the adsorption of SMX on SB by 21.5%, while the presence of IBU decreased the adsorption by 23%. This result demonstrates the competition for the active sites for all drugs and the similar affinity of IBU and DCF for bagasse. The decrease in SMX adsorption was stronger at high concentrations. The capacity of adsorption was reduced by 33%, especially in the presence of IBU. In any case, when increasing the concentration solution, the adsorption of each drug increased due to its adsorption in multilayers.

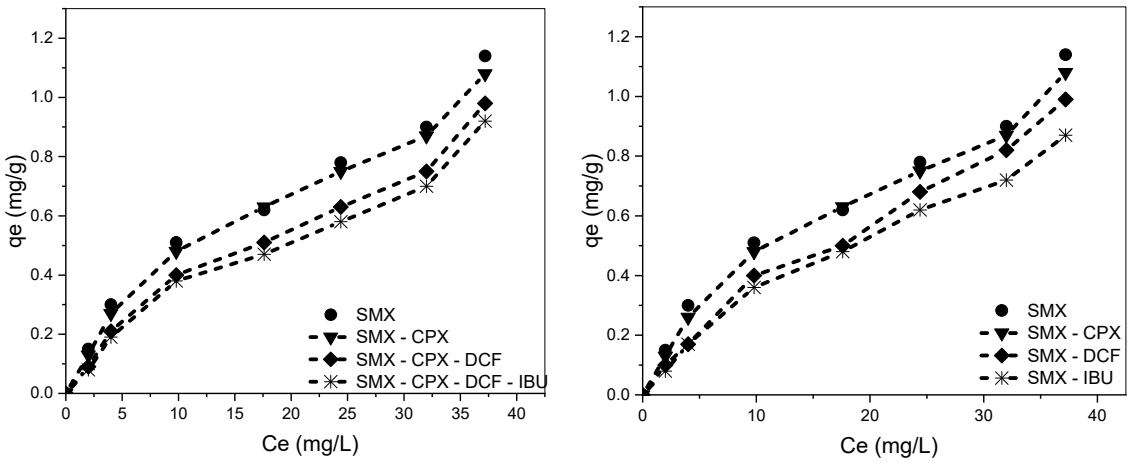

Figure 7. (**a**) SMX experimental isotherms in multi-component mixtures and (**b**) SMX experimental isotherms in bi-component mixtures.

In ternary mixtures (DCF, SMX, and IBU), DCF adsorption decreased between 8.5 and 27.8%, as shown in Figure S2a. The presence of CPX did not decrease the adsorption of DCF; therefore CPX did not influence its adsorption. As shown in Figure S2b, IBU had more influence on the decrease in the adsorption amount of DCF. Both drugs, DCF and IBU, had a similar affinity for bagasse; consequently, they competed for active sites. Compared with adsorption for individual DCF, the capacity of adsorption decreased by 12.6 to 28.3% with DCF and IBU and by 8.1 to 24.64% with DCF and SMX simultaneously.

Figure S3 shows the adsorption isotherms of IBU in combination with the other drugs studied. The ternary and quaternary simultaneous systems showed a decrease in comparison to the single component, while CPX did not have an influence on IBU adsorption (Figure S3a). The interpretation is the same as that for DCF and SMX, as discussed above. The adsorption amounts of IBU were IBU singly, IBU with CPX, IBU with SMX, and SMX with DCF (Figure S3b). These results indicated greater competition between DCF and IBU (Figure 5b), suggesting that the presence of DCF significantly decreased IBU adsorption.

It is known that the adsorption potential increases with decreasing pore size [34]. SB is macroporous; therefore, the quantity of active sites with high adsorption potential is low. These sites are occupied by the drug with the highest affinity, in this case, CPX, leaving fewer adsorption sites available for molecules with lower affinity (DCF > IBU > SMX) [35] and causing competition between the drugs for the sites that become available.

The low specific surface area of SB makes competition for adsorption sites evident, especially at high concentrations [32]. However, the adsorbed drugs could serve as new active sites for adsorption.

At the experimental pH of 6.5, SB had a slight positive charge (pH_{ZCP} 5.9), while DCF, SMX, and IBU had a negative charge, suggesting an electrostatic interaction between SB and DCF and IBU. CPX was in the zwitterionic form; consequently, electrostatic interaction was low.

In all cases, there were other interactions between SB and drugs. These mechanisms can be as follows:

(1) Polar groups present in the drugs, such as F, Cl, N, and O, and those in SB form hydrogen bonds and dipole attractions [10,36].
(2) Functional groups such as NH and OH occur in the drugs and behave as donors, while benzene rings act as receptors for hydrogen bonds [37].
(3) π-π bonds [38].
(4) Dipole attraction [39–41].

Lignin contains functional groups of hydrogen and oxygen that allow the formation of hydrogen bonds with drugs (Figure 8). Electronegative atoms of drugs (F, O, or N) form dipole–dipole bonds with the H of lignin and cellulose.

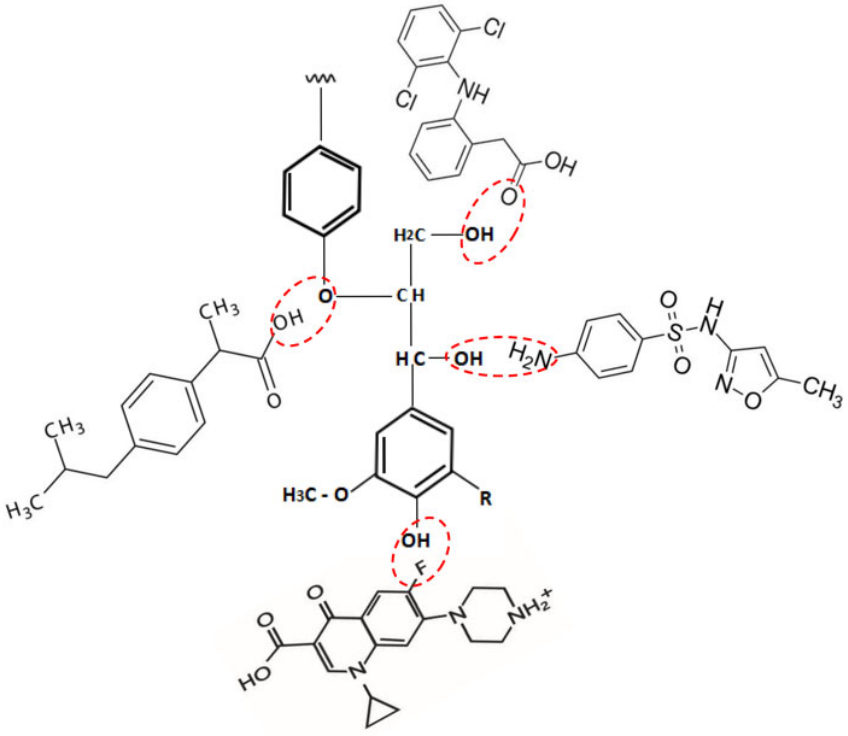

Figure 8. Hydrogen bonds between drugs and lignin.

These mechanisms are the same for the adsorption of CPX, SMX, DCF, and IBU, resulting in competition between them due to the H of SB. The presence of the F in CPX makes the unions of CPX and SB stronger.

The results show that the presence of the drugs SXM, DCF, and IBP does not influence the adsorption of CPX; therefore, CPX adsorption can be estimated by its single component isotherm. All other drugs have a greater or lesser impact on the adsorption of others [42].

3.5. Influence of the Amount of Each Drug

To determine the competition among individual solutes regarding the adsorption of other drugs onto SB, the concentration of one adsorbate was varied while the amount of the other was held constant. Therefore, for an SMX–DCF system, the initial concentrations of DCF varied from 5 to 50 mg/L, while the initial concentration of SMX was always 20 mg/L.

Figure 9 shows the competitive adsorption at different concentrations between SMX vs. CPX, DCF, and IBU (Figure 9a), DCF vs. SMX, CPX, and IBU (Figure 9b), and IBU vs. DCF, CPX, and SMX (Figure 9c).

The competition of other drugs with DCF followed the order IBU > DCF > CPX. In this system, as in other systems, the interaction strength between CPX and SB did not decrease during competitive adsorption in the presence of other drugs. The amount adsorbed was lower at higher concentrations of the competitive drug. This behavior was similar to that of the other drugs.

For binary, ternary, and quaternary simultaneous systems, the total amount of drugs adsorbed by SB was greater than the amount of drug adsorbed as a single solute. For example, for a quaternary system (initial concentration of 20 mg/L), the total amount adsorbed by SB of all drugs was 2.41 mg/g. This indicates that an interaction of the drugs among themselves. For example, the adsorbed SMX molecules function as new active sites to adsorb more SMX. It should also be considered that adsorption on bagasse

occurs in a multilayer [10]. Binding between drugs forming complexes is also possible. Therefore, in the adsorption of drugs on SB, the interactions between the solutes cannot be neglected. That implies that the Langmuir extension equation proposed by Markham and Benton for multi-solutes cannot be applied since it assumes that the only competitive effect is due to the reduction of the number of active sites for adsorption [42]. In the study carried out by Vijayaraghavan and Balasubramanian [43], the SRS equation showed a more precise adjustment of data in binary adsorption onto crab shells. For that, the data of bi-component solutions in this study were adjusted to the Sheindorf–Rebhun–Sheintuch model. SRS proposes that the value of $\alpha_{i,j}$ ranges from 0 to 10. A lower value indicates lower competition. For the binary systems, i.e., SMX with CPX, DCF with CPX, and IBU with CPX, the values of the competition factor α2,1 were 0.43, 0.35, and 0.41, confirming that CPX does not have an effect on the adsorption of other drugs.

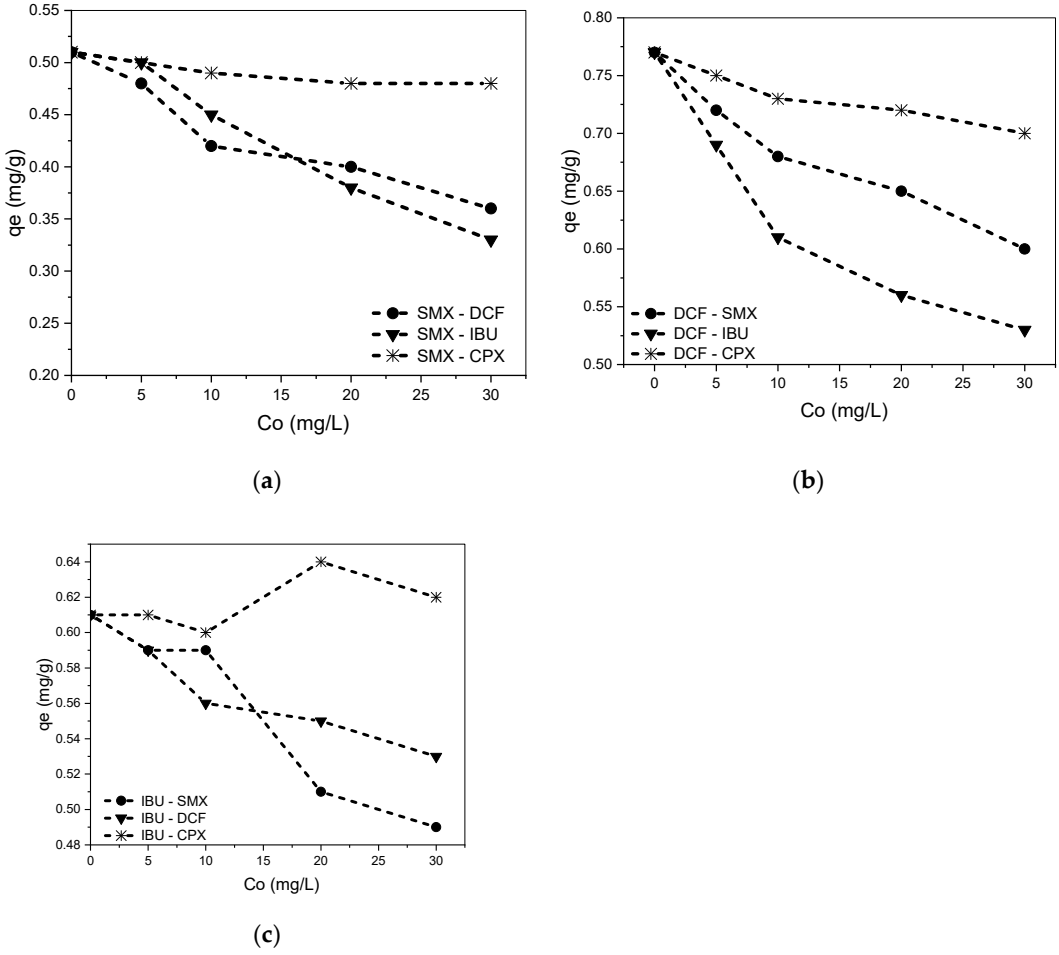

Figure 9. Amount of drug adsorbed onto SB in binary mixtures at different concentrations. (**a**) SMX, (**b**) DCF, and (**c**) IBU.

For bi-component experimental data SMX with DCF, the competition factor $\alpha_{1,2}$ was 1.32, while $\alpha_{2,1}$ was 0.75. As can see from the experimental data, there was greater competition between SMX over DCF than between DCF over SMX adsorption [34,44]. For the bi-component system, DCF − IBU $\alpha_{1,2}$ = 1.09 y $\alpha_{2,1}$ = 0.90, showing low competition between them, as also observed in the experimental data.

Figure 10a illustrates the experimental and calculated isotherms of the bi-component DCF–IBU system based on the SRS model with R^2 = 0.94. The experimental and calculated CPX–SMX adsorption isotherms are shown in Figure 10b, and a value of R^2 = 0.97 was obtained. Therefore, the SRS model was able to predict the studied bi-component adsorption of this work. The SRS model has been efficaciously used in fitting other bi-component

systems such as caffeine–diclofenac [34]; 4-nitrophenol, and basic yellow 28 dye over montmorillonite [45], and 4-nitrophenol and 2-nitrophenol on activated carbon [46].

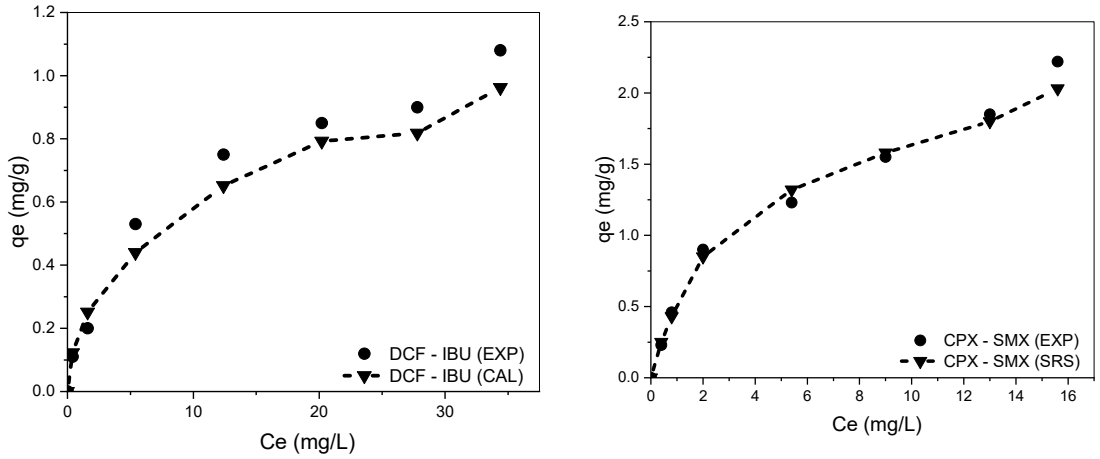

Figure 10. Adsorption isotherms, (**a**) DCF–IBU adsorption isotherm; (**b**) CPX–SMX adsorption isotherm.

3.6. Espectro FTIR

Based on the FTIR spectrum before and after the adsorption process was determined, the functional groups present in the SB were as follows: O-H (3335 cm^{-1}), C-H (2890 cm^{-1}), C=O (1726 cm^{-1}), C=C (1603 cm^{-1}), C-H (1425 cm^{-1}), C–O (1370 cm^{-1}), O-H (1319 cm^{-1}), C-O-C, C-O (1240 cm^{-1}), C-O-C, C-OH (1160 cm^{-1}), C-H (900–800 cm^{-1}). After adsorption, between 1500 and 1750 cm^{-1}, new peaks were observed that corresponded to the union of bagasse with CPX as shown in Figure S4.

4. Conclusions

Competitive adsorption studies show the viability of sugarcane bagasse to remove CPX, DCF, SMX, and IBU from single-component and simultaneous multi-component systems.

In the single-component adsorption, high removal of CPX was observed compared to that reached with the other drugs (DCF, SMX, and IBU). The low SMX adsorption capacity (0.51 m/g) showed it to be the least favorable solute for adsorption onto SB. In addition, the amount of SMX adsorbed was low in the presence of other drugs, while the capacity of SB to adsorb CPX did not decrease throughout competitive adsorption. CPX reached a capacity of 0.98 mg/g and was almost constant, even in the presence of the other pharmaceuticals.

The other multi-component systems (without CPX) led to lower adsorption capacities than those obtained with single components, demonstrating competition for the available adsorption sites. The greatest competitive effect occurred between DCF and IBU since the two have a similar affinity for SB.

All bi-component experimental data fit better to the SRS model, indicating that the decrease in the adsorbed amounts was due to interaction between solutes and competition for active sites. The competitive effect was high at higher concentrations due to the saturation of the active sites, which were low in number due to the low specific surface of the SB. However, despite its low adsorption capacity, SB can be used as an adsorbent due to its low cost, high availability, and the possibility of environmentally compatible final disposal.

Supplementary Materials: The following supporting information can be downloaded at: https://www.mdpi.com/article/10.3390/w15112127/s1; HPLC procedure: The concentration and absorptivity coefficients obtained were verified using high-efficiency liquid chromatography on the YL Instrument 9300 HPLC System coupled with a diode UV–VIS, with a Zorbax SB-C18 column. The temperature of the column was set at 25 °C. The mobile phases were (A) water/ACN 66.6:33.3 *v*/*v* acidified with ortho-phosphoric acid 85% to pH 2.7 and (B) pure ANC. The elution gradient was programmed as starting from 20% B for 3 min to 65% B by 7 min; this concentration was maintained until 10 min and then it was increased to 100% B in 2 min. It returned to initial conditions until 15 min. The posting time was set at 3 min to allow column equilibrium to be reached. Figure S1. Percentage removal of IBU, DCF, SMX, and CPX with 20 mg/L of SB. Figure S2. (a) DCF experimental isotherms in multi-component mixtures and (b) DCF experimental isotherms in bi-component mixtures. Figure S3. (a) IBU experimental isotherms in multi-component mixtures and (b) IBU experimental isotherms in bi-component mixtures. Figure S4. FTRI spectrum.

Author Contributions: Conceptualization, methodology, software, M.E.P.; validation, formal analysis, investigation, resources, data curation, writing—original draft preparation, writing—review and editing, visualization, M.E.P. and D.F.; supervision, project administration, funding acquisition, M.E.P. All authors have read and agreed to the published version of the manuscript.

Funding: This research received no external funding.

Data Availability Statement: Not applicable.

Acknowledgments: The authors would like to acknowledge the Facultas de Ciencias Químicas de la Universidad de Cuenca, the Vicerrectorado de Investigación de la Universidad de Cuenca, and the use of the Servicio General de Apoyo a la investigación-SAI, Universidad de Zaragoza.

Conflicts of Interest: The authors declare no conflict of interest.

References

1. Bilal, M.; Adeel, M.; Rasheed, T.; Zhao, Y.; Iqbal, H.M. Emerging contaminants of high concern and their enzyme-assisted biodegradation—A review. *Environ. Int.* **2019**, *124*, 336–353. [CrossRef]
2. Felis, E.; Kalka, J.; Sochacki, A.; Kowalska, K.; Bajkacz, S.; Harnisz, M.; Korzeniewska, E. Antimicrobial pharmaceuticals in the aquatic environment-occurrence and environmental implications. *Eur. J. Pharmacol.* **2020**, *866*, 172813. [CrossRef] [PubMed]
3. Kutuzova, A.; Dontsova, T.; Kwapinski, W. Application of TiO_2-Based Photocatalysts to Antibiotics Degradation: Cases of Sulfamethoxazole, Trimethoprim and Ciprofloxacin. *Catalysts* **2021**, *11*, 728. [CrossRef]
4. Tran, N.H.; Reinhard, M.; Gin, K.Y.H. Occurrence and fate of emerging contaminants in municipal wastewater treatment plants from different geographical regions—A review. *Water Res.* **2018**, *133*, 182–207. [CrossRef]
5. Wilkinson, J.; Hooda, P.S.; Barker, J.; Barton, S.; Swinden, J. Occurrence, fate and transformation of emerging contaminants in water: An overarching review of the field. *Environ. Pollut.* **2017**, *231*, 954–970. [CrossRef] [PubMed]
6. Kaya, G.G.; Aznar, E.; Deveci, H.; Martínez-Máñez, R. Low-cost silica xerogels as potential adsorbents for ciprofloxacin removal. *Sustain. Chem. Pharm.* **2021**, *22*, 100483.
7. Ramírez-Malule, H.; Quiñones-Murillo, D.H.; Manotas-Duque, D. Emerging contaminants as global environmental hazards. A bibliometric analysis. *Emerg. Contam.* **2020**, *6*, 179–193. [CrossRef]
8. Silva, C.P.; Jaria, G.; Otero, M.; Esteves, V.I.; Calisto, V. Waste-based alternative adsorbents for the remediation of pharmaceutical contaminated waters: Has a step forward already been taken? *Bioresour. Technol.* **2018**, *250*, 888–901. [CrossRef]
9. Peñafiel, M.E.; Matesanz, J.M.; Vanegas, E.; Bermejo, D.; Ormad, M.P. Corncobs as a potentially low-cost biosorbent for sulfamethoxazole removal from aqueous solution. *Sep. Sci. Technol.* **2020**, *55*, 3060–3071. [CrossRef]
10. Peñafiel, M.E.; Matesanz, J.M.; Vanegas, E.; Bermejo, D.; Mosteo, R.; Ormad, M.P. Comparative adsorption of ciprofloxacin on sugarcane bagasse from Ecuador and on commercial powdered activated carbon. *Sci. Total Environ.* **2021**, *750*, 141498. [CrossRef]
11. Fan, X.; Deng, L.; Li, K.; Lu, H.; Wang, R.; Li, W. Adsorption of malachite green in aqueous solution using sugarcane bagasse-barium carbonate composite. *Colloid Interface Sci. Commun.* **2021**, *44*, 100485. [CrossRef]
12. Sharma, B.M.; Bečanová, J.; Scheringer, M.; Sharma, A.; Bharat, G.K.; Whitehead, P.G.; Nizzetto, L. Health and ecological risk assessment of emerging contaminants (pharmaceuticals, personal care products, and artificial sweeteners) in surface and groundwater (drinking water) in the Ganges River Basin, India. *Sci. Total Environ.* **2019**, *646*, 1459–1467. [CrossRef] [PubMed]
13. Dhiman, N.; Sharma, N. Removal of pharmaceutical drugs from binary mixtures by use of ZnO nanoparticles:(Competitive adsorption of drugs). *Environ. Technol. Innov.* **2019**, *15*, 100392. [CrossRef]
14. Jung, C.; Boateng, L.K.; Flora, J.R.; Oh, J.; Braswell, M.C.; Son, A.; Yoon, Y. Competitive adsorption of selected non-steroidal anti-inflammatory drugs on activated biochars: Experimental and molecular modeling study. *Chem. Eng. J.* **2015**, *264*, 1–9. [CrossRef]

15. Li, Z.; Wang, Z.; Wu, X.; Li, M.; Liu, X. Competitive adsorption of tylosin, sulfamethoxazole and Cu (II) on nano-hydroxyapatitemodified biochar in water. *Chemosphere* **2020**, *240*, 124884. [CrossRef] [PubMed]
16. Li, X.; Kuang, Y.; Chen, J.; Wu, D. Competitive adsorption of phosphate and dissolved organic carbon on lanthanum modified zeolite. *J. Colloid Interface Sci.* **2020**, *574*, 197–206. [CrossRef]
17. Zainab, S.M.; Junaid, M.; Xu, N.; Malik, R.N. Antibiotics and antibiotic resistant genes (ARGs) in groundwater: A global review on dissemination, sources, interactions, environmental and human health risks. *Water Res.* **2020**, *187*, 116455. [CrossRef] [PubMed]
18. Khamash, D.F.; Voskertchian, A.; Tamma, P.D.; Akinboyo, I.C.; Carroll, K.C.; Milstone, A.M. Increasing clindamycin and trimethoprim-sulfamethoxazole resistance in pediatric *Staphylococcus aureus* infections. *J. Pediatr. Infect. Dis. Soc.* **2019**, *8*, 351–353. [CrossRef]
19. Serwecińska, L. Antimicrobials and antibiotic-resistant bacteria: A risk to the environment and to public health. *Water* **2020**, *12*, 3313. [CrossRef]
20. Brown, J.N.; Paxéus, N.; Förlin, L.; Larsson, D.J. Variations in bioconcentration of human pharmaceuticals from sewage effluents into fish blood plasma. *Environ. Toxicol. Pharmacol.* **2007**, *24*, 267–274. [CrossRef]
21. Schwaiger, J.; Ferling, H.; Mallow, U.; Wintermayr, H.; Negele, R.D. Toxic effects of the non-steroidal anti-inflammatory drug diclofenac: Part I: Histopathological alterations and bioaccumulation in rainbow trout. *Aquat. Toxicol.* **2004**, *68*, 141–150. [CrossRef]
22. Worch, E. Adsorption equilibrium II: Multisolute adsorption. In *Adsorption Technology in Water Treatment*; De Gruyter: Berlin, Germany, 2012.
23. DiGiano, F.A.; Baldauf, G.; Frick, B.; Sontheimer, H. A simplified competitive equilibrium adsorption model. *Chem. Eng. Sci.* **1978**, *33*, 1667–1673. [CrossRef]
24. Sheindorf, C.H.; Rebhun, M.; Sheintuch, M. A Freundlich-type multicomponent isotherm. *J. Colloid Interface Sci.* **1981**, *79*, 136–142. [CrossRef]
25. Gutierrez, M.; Fuentes, H.R. Modeling adsorption in multicomponent systems using a Freundlich-type isotherm. *J. Contam. Hydrol.* **1993**, *14*, 247–260. [CrossRef]
26. Linares, R.V.; Yangali-Quintanilla, V.; Li, Z.; Amy, G. Rejection of micropollutants by clean and fouled forward osmosis membrane. *Water Res.* **2011**, *45*, 6737–6744. [CrossRef] [PubMed]
27. Doğan, E.C. Investigation of ciprofloxacin removal from aqueous solution by nanofiltration process. *Glob. NEST J.* **2016**, *18*, 291–308.
28. Varma, A.K.; Mondal, P. Physicochemical characterization and pyrolysis kinetic study of sugarcane bagasse using thermogravimetric analysis. *J. Energy Resour. Technol.* **2016**, *138*, 052205. [CrossRef]
29. Carrier, M.; Joubert, J.E.; Danje, S.; Hugo, T.; Görgens, J.; Knoetze, J.H. Impact of the lignocellulosic material on fast pyrolysis yields and product quality. *Bioresour. Technol.* **2013**, *150*, 129–138. [CrossRef]
30. Abdolali, A.; Guo, W.S.; Ngo, H.H.; Chen, S.S.; Nguyen, N.C.; Tung, K.L. Typical lignocellulosic wastes and by-products for biosorption process in water and wastewater treatment: A critical review. *Bioresour. Technol.* **2014**, *160*, 57–66. [CrossRef]
31. Carrott, P.J.M.; Carrott, M.R. Lignin–from natural adsorbent to activated carbon: A review. *Bioresour. Technol.* **2007**, *98*, 2301–2312.
32. Mansouri, H.; Carmona, R.J.; Gomis-Berenguer, A.; Souissi-Najar, S.; Ouederni, A.; Ania, C.O. Competitive adsorption of ibuprofen and amoxicillin mixtures from aqueous solution on activated carbons. *J. Colloid Interface Sci.* **2015**, *449*, 252–260. [CrossRef] [PubMed]
33. Giles, C.H.; Smith, D.; Huitson, A. A general treatment and classification of the solute adsorption isotherm. I. Theoretical. *J. Colloid Interface Sci.* **1974**, *47*, 755–765. [CrossRef]
34. Sotelo, J.L.; Ovejero, G.; Rodríguez, A.; Álvarez, S.; Galán, J.; García, J. Competitive adsorption studies of caffeine and diclofenac aqueous solutions by activated carbon. *Chem. Eng. J.* **2014**, *240*, 443–453. [CrossRef]
35. Pelekani, C.; Snoeyink, V.L. Competitive adsorption in natural water: Role of activated carbon pore size. *Water Res.* **1999**, *33*, 1209–1219. [CrossRef]
36. Bhadra, B.N.; Seo, P.W.; Jhung, S.H. Adsorption of diclofenac sodium from water using oxidized activated carbon. *Chem. Eng. J.* **2016**, *301*, 27–34. [CrossRef]
37. Afzal, M.Z.; Sun, X.F.; Liu, J.; Song, C.; Wang, S.G.; Javed, A. Enhancement of ciprofloxacin sorption on chitosan/biochar hidrogel beads. *Sci. Total Environ.* **2018**, *639*, 560–569. [CrossRef]
38. Li, X.; Chen, S.; Fan, X.; Quan, X.; Tan, F.; Zhang, Y.; Gao, J. Adsorption of ciprofloxacin, bisphenol and 2-chlorophenol on electrospun carbon nanofibers: In comparison with powder activated carbon. *J. Colloid Interface Sci.* **2015**, *447*, 120–127. [CrossRef] [PubMed]
39. Ngo, H.H.; Guo, W.; Zhang, J.; Liang, S.; Ton-That, C.; Zhang, X. Typical low-cost biosorbents for adsorptive removal of specific organic pollutants from water. *Bioresour. Technol.* **2015**, *182*, 353–363.
40. Rosales, E.; Meijide, J.; Pazos, M.; Sanromán, M.A. Challenges and recent advances in biochar as low-cost biosorbent: From batch assays to continuous-flow systems. *Bioresour. Technol.* **2017**, *246*, 176–192. [CrossRef]
41. Tonucci, M.C.; Gurgel, L.V.A.; de Aquino, S.F. Activated carbons from agricultural byproducts (pine tree and coconut shell), coal, and carbon nanotubes as adsorbents for removal of sulfamethoxazole from spiked aqueous solutions: Kinetic and thermodynamic studies. *Ind. Crops Prod.* **2015**, *74*, 111–121. [CrossRef]

42. Seader, J.D.; Henley, E.J.; Roper, D.K. Adsorption, Ion Exchange, Chromatography, and Electrophoresis. In *Separation Process Principles*, 3rd ed.; John Wiley & Sons, Inc.: New York, NY, USA, 1998; Volume 25, pp. 568–648.
43. Vijayaraghavan, K.; Balasubramanian, R. Single and binary biosorption of cerium and europium onto crab shell particles. *Chem. Eng. J.* **2010**, *163*, 337–343. [CrossRef]
44. Wu, C.H.; Kuo, C.Y.; Lin, C.F.; Lo, S.L. Modeling competitive adsorption of molybdate, sulfate, selenate, and selenite using a Freundlich-type multi-component isotherm. *Chemosphere* **2002**, *47*, 283–292. [CrossRef] [PubMed]
45. Zermane, F.; Bouras, O.; Baudu, M.; Basly, J.P. Cooperative coadsorption of 4-nitrophenol and basic yellow 28 dye onto an iron organo–inorgano pillared montmorillonite clay. *J. Colloid Interface Sci.* **2010**, *350*, 315–319. [CrossRef] [PubMed]
46. Hamidouche, S.; Bouras, O.; Zermane, F.; Cheknane, B.; Houari, M.; Debord, J.; Baudu, M. Simultaneous sorption of 4-nitrophenol and 2-nitrophenol on a hybrid geocomposite based on surfactant-modified pillared-clay and activated carbon. *Chem. Eng. J.* **2015**, *279*, 964–972. [CrossRef]